Liew, C. C., Haslet, G. W., and Allfrey, V. G. (1970), *Nature (London) 226,* 414.
Marchis-Mouren, G., and Lipmann, F. (1965), *Proc. Natl. Acad. Sci. U.S.A. 53,* 1147.
Maszluff, W. F., and McCarty, K. S. (1970), *J. Biol. Chem. 245,* 5635.
Menninger, J. R., Deery, S., Draper, D., and Walker, Ch. (1974), *Biochim. Biophys. Acta 335,* 185.
Pestana, A., and Pitot, H. C. (1973), *Fed. Proc., Fed. Am. Soc. Exp. Biol. 57,* 583.
Pestana, A., and Pitot, H. C. (1974) *Nature (London) 247,* 200.
Pestana, A., and Pitot, H. C. (1975) *Biochemistry,* preceding paper.
Pestana, A., Sudilovsky, O., and Pitot, H. C. (1971), *FEBS Lett. 19,* 83.
Shih, D. S., and Kaesberg, P. (1973), *Proc. Natl. Acad. Sci. U.S.A. 70,* 1799.
Strous, G. J. A. M., Berns, A. J. M., and Bloemendal, H. (1974), *Biochem. Biophys. Res. Commun. 58,* 876.
Strous, G. J. A. M., van Westreenen, H., and Bloemendal, H. (1973), *Eur. J. Biochem. 38,* 79.
Venkatesan, N., and Steele, W. J. (1972), *Biochim. Biophys. Acta 287,* 526.

Comparative Ability of RNA and DNA to Prime DNA Synthesis in Vitro: Role of Sequence, Sugar, and Structure of Template · Primer†

Toby M. Tamblyn and Robert D. Wells*

ABSTRACT: The priming efficiency of oligo(RNA) vs. oligo(DNA) in a homopolymer template · homooligomer primer system was compared using four DNA polymerases. The templates included $(dT)_n$, $(dA)_n$, $(dC)_n$, and $(dI)_n$. Primers were the oligomers of the complementary DNA or RNA with chain lengths of 6 to 23. The DNA polymerases used were from *Micrococcus luteus,* avian myeloblastosis virus (AMV), and *Escherichia coli* (polymerase I and polymerase III). The polymerases demonstrated a preference for the DNA primers with $(dC)_n$, $(dA)_n$, and $(dI)_n$ templates. However, when $(dT)_n$ was the template, all but the AMV polymerase preferred $(rA)_{11}$ more than 200-fold better than $(dA)_{12}$. This preference was due to the physical structure of the initiation complex. The structures of the oligo · polymer complexes were characterized by mixing curves, melting curves, and analytical buoyant density analyses. $(rA)_{11} + (dT)_n$ formed predominantly a duplex structure, whereas $(dA)_{12} + (dT)_n$ formed the three-stranded structure, $(dA)_{12} \cdot 2(dT)_n$. The K_m of the duplex with *E. coli* Pol III was 2.9 μM $(rA)_{11}$. The K_i of the triplex was 2.2 μM $(dA)_{12}$, indicating that Pol III could bind to the triplex but would not elongate the $(dA)_{12}$ primer. The influence of structure on priming also was demonstrated with longer oligomers, $(dA)_{23}$ and $(rA)_{23}$, where the $(dA)_{23}$ formed more duplex-like structures and primed more than the $(dA)_{12}$. $(dT)_{10} + (dA)_n$ complexes also were shown to form triplex structures that inhibited priming. These results show that template · primer structure has more influence on priming than the sugar moiety or the sequence of the nucleic acid.

Prior studies from this and other laboratories (Green and Gerard, 1974) were aimed at establishing the specificities for template · primers of DNA polymerases isolated from several different sources. Studies were performed with polymeric DNAs, RNAs, and DNA · RNA hybrids as well as with natural nucleic acids. These studies documented that DNA polymerases are qualitatively similar in their requirements but that quantitative differences existed in their capacities to utilize certain template · primers. Bacterial DNA polymerases as well as the "reverse transcriptase" from AMV[1] had a pronounced preference for DNA rather than RNA templates (Green and Gerard, 1974) except in certain cases when deoxyribooligonucleotide primers were utilized (Baltimore and Smoler, 1971; Goodman and Spiegelman, 1971; Wells et al., 1972).

Prior studies from this and other laboratories also have demonstrated that RNA, as well as DNA, can serve as a primer for DNA synthesis in vitro and in vivo (for a review see Wells and Inman, 1973). Early reports showed a stimulatory role for RNA (suggesting its role as primer); more convincingly, recent work provided direct chemical analyses of the RNA–DNA covalent bonds formed at the initiation site (Wells et al., 1972; Leis and Hurwitz, 1972; Flügel and Wells, 1972; Keller, 1972; Verma et al., 1972, and later papers). In those cases where the homologous high molecular weight RNAs and DNAs were compared as primers, the RNAs generally primed as well (Wells et al., 1972) or a little less efficiently (Chang and Bollum, 1972) than the DNAs.

We wished to compare further the ability of RNA and DNA to serve as primer for DNA synthesis in vitro in well-characterized systems. Since a goal was to quantitate initial

† From the Department of Biochemistry, College of Agricultural and Life Sciences, University of Wisconsin, Madison, Wisconsin 53706. *Received November 13, 1974.* This work was supported by funds from the National Institutes of Health (CM-12275) and the National Science Foundation (BMS74-21420).

[1] Abbreviations used are: AMV, avian myeloblastosis virus; Pol I, *Escherichia coli* DNA polymerase I (polA); Pol III, *E. coli* DNA polymerase III (polC or dnaE).

kinetic rates, short-chain ribo- and deoxyribonucleotide primers were used since it was possible to accurately determine their chain length, and hence the number of 3′-OH ends in a reaction. Also, as mentioned above, certain deoxyribooligonucleotide primers seemed to emphasize the specificity of some polymerases; however, no systematic studies had been performed with ribooligonucleotide primers.

Figure 1 shows a generalized scheme for the assays. A homopolymer combined with a complementary homooligomer was used as template · primer for the incorporation of dMMP which was complementary to the template. The four highly purified DNA polymerases studied were a "reverse transcriptase" from an RNA tumor virus, two apparent "repair" enzymes, and a polymerase with a genetically established role in chromosomal replication. In some cases where unusual priming abilities were observed, the polymer · oligomer complexes were studied physically to determine their structures and structural transitions induced by temperature under the polymerase assay conditions.

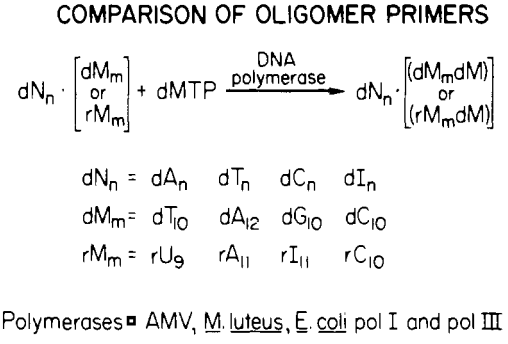

FIGURE 1: Scheme of polymerase assays.

Materials and Methods

Nucleic Acids. Nonradioactive and labeled deoxytriphosphates were purchased and characterized in chromatographic systems A and B as previously described (Burd and Wells, 1970). In virtually all cases, the nucleotides were at least 80% pure. DNA and RNA polymers were prepared and characterized as described (Wells et al., 1972). [8-^{3}H](rA)$_n$ (10 μCi/μmol) was purchased from Miles Laboratories. (dA)$_8$, (dA)$_{12-18}$, (dC)$_{10}$, and (dG)$_{10}$ were purchased from Collaborative Research, Inc. The following oligomers were gifts: (dT)$_{10}$ and (dT)$_{11}$ from R. W. Sweet (this laboratory); (rC)$_6$ and (rU)$_7$ from Robert Thach, Washington University; (rU)$_9$ from Gunther Weimann, Boehringer Mannheim GMBH, Tutzing, Germany; (rI)$_{11}$ from Paul Ts'o, Johns Hopkins University; and (rA)$_8$ from Uttam RajBhandary, Massachusetts Institute of Technology. These oligomers were characterized by descending chromatography on prewashed Whatman No. 3MM paper in system C. The oligomers were separated from salt and impurities from the paper chromatography step by Bio-Gel P2 column chromatography. The oligomer extinction coefficients used were those reported previously for (dC)$_m$ and (rC)$_m$ (Adler et al., 1967), for (dA)$_m$ and (dT)$_m$ (Cassani and Bollum, 1969), and (rA)$_m$ (Uhlenbeck, 1969). Polymer extinction coefficients were used for oligomers with m greater than 20 and for (dG)$_{10}$ and (rI)$_{11}$ (Chamberlin and Patterson, 1965; Riley et al., 1966). To ensure that the oligomer preparations did not contain a nonspecific inhibitor for the DNA polymerase reaction, the oligomers were added at 24 μM to a (dA-dT)$_n$ · (dA-dT)$_n$ primed reaction with *M. luteus* DNA polymerase; no inhibition was observed.

(rA)$_{11}$ and other short-chain oligo(rA)'s of varying chain lengths were prepared by limited alkaline digestion of (rA)$_n$ essentially as described previously (Uhlenbeck, 1969). The extent of hydrolysis was monitored qualitatively by descending paper chromatography in systems C and D. For a large scale preparation, 92 mg of (rA)$_n$, including 10 μCi [8-^{3}H](rA)$_n$, was digested at 30 mg/ml in 1 N KOH for 25 min at 37°. The hydrolysis mixture was neutralized with Dowex 50-H$^+$. Subsequent bacterial alkaline phosphatase (hereafter referred to as phosphatase) treatment was similar to that previously described (Weiss et al., 1968). The digest was then fractionated by TEAE-cellulose chromatography which resolved 12 peaks after the void volume. The chain lengths of two of the peaks were determined by nucleotide/nucleoside ratios; total digestion was with alkali and, separately, with venom phosphodiesterase. The average of the results from the two types of determinations indicated that peak 6 after the void volume was the 6-mer and that peak 9 was the 9-mer. Further confirmation of the length of the oligo(rA)'s was obtained on analytical polyacrylamide gels (Burd and Wells, 1974).

For the preparation of (rA)$_{23}$, (rA)$_n$ was digested with alkali by the procedure described above. The incubation time necessary to maximize production of (rA)$_{25}$ was determined by analytical polyacrylamide gel electrophoresis of the product of a small scale reaction. Oligomers from a large scale digestion were fractionated on preparative polyacrylamide gels (Burd and Wells, 1974). The isolated oligomer pools then were treated with phosphatase to remove 3′-phosphates and their chain length was determined on analytical gels. The (rA)$_{23}$ pool contained predominantly the 23-mer as well as (rA)$_{22}$ and (rA)$_{24}$ (approximately 30% each).

(dA)$_{23}$ and other large oligo(dA)'s were prepared by limited digestion of (dA)$_n$ with pancreatic DNase as described previously (Burd and Wells, 1974). The reaction conditions were 10 A_{260} units/ml of (dA)$_n$, 50 mM Tris-HCl (pH 7.8), 1 mM $MnCl_2$, and 0.016 mg/ml of DNase in a 20-ml volume. Conditions for optimal production of (dA)$_{20-30}$ were determined to be 15 min at 37° by small scale reactions followed by analytical gels. The reaction was stopped by addition of EDTA to 5 mM and the solution was heated at 65° for 10 min. The digest was fractionated on a preparative gel essentially as described for (rA)$_{23}$. The distribution of oligomers across the gel was determined by analytical gels. The (dA)$_{23}$ pool also contained (dA)$_{22}$ and (dA)$_{24}$.

(rC)$_{10}$ was prepared by alkaline digestion of (rC)$_n$ and preparative polyacrylamide electrophoresis served to fractionate the oligomers as described above.

Conditions for Comparative DNA Polymerase Assays. For the AMV DNA polymerase, the reaction mixtures (0.05 or 0.15 ml) consisted of 50 mM Tris-HCl (pH 8.1), 5 mM $MgCl_2$, 10 mM dithiothreitol, 0.06 mM dMTP[2] including ^{3}H- or α-^{32}P-labeled dMTP, 0.03 mM (dN)$_n$,[2] and oligomer, (dM)$_m$,[2] as indicated. For the *M. luteus* DNA polymerase and the Pol I, the reaction mixtures (0.15 ml) contained 50 mM Tris-HCl (pH 8.1), 10 mM $MgCl_2$, 20

[2] Nomenclature of nucleic acids and precursors is that designated by the IUPAC-IUB Commission on Biochemical Nomenclature [*Biochemistry 9*, 4022 (1970)] except that the deoxynucleotide triphosphates and deoxynucleotide product are designated as dMTP and (dM)$_m$ to emphasize their complementarity to the template, (dN)$_n$. Subscripts n and m designate polymer length above 100 nucleotides and oligomer length below 50 nucleotides, respectively.

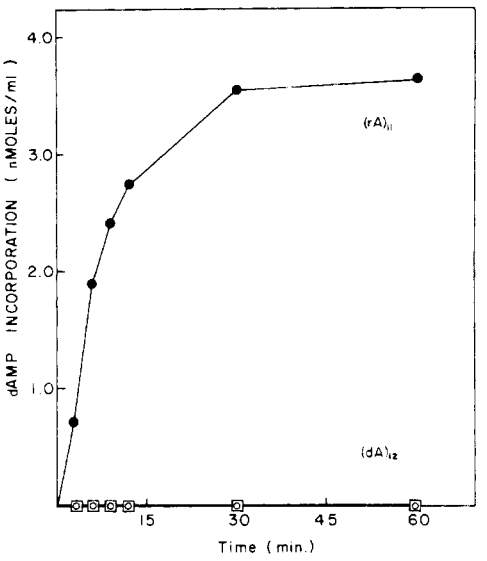

FIGURE 2: Ability of $(rA)_{11}$ and $(dA)_{12}$ to prime $(dT)_n$-templated reactions with Pol III in MME buffer. The conditions were those described in Materials and Methods. The concentration of $(dT)_n$ was 24 μM and that of $(dA)_{12}$ and $(rA)_{11}$ was 12 μM. Pol III was used at 0.56 μg/0.150 ml reaction volume at 25°. Specific activity of the [α-^{32}P]dATP was 0.94 pmol/ml per cpm: (□) no oligomer added; (○) plus $(dA)_{12}$; (●) plus $(rA)_{11}$.

mM β-mercaptoethanol, 0.12 mM dMTP (including ^{3}H or α-^{32}P-labeled dMTP), 0.024 mM $(dN)_n$, and oligomer $(dM)_m$ as indicated. This buffer system is designated as TM. Reaction conditions for Pol III were as described (Kornberg and Gefter, 1972): 33 mM morpholinopropanesulfonate-KOH (pH 7.0); 13 mM $MgCl_2$; 48 mM β-mercaptoethanol; 10% ethanol; 0.12 mM dMTP (including ^{3}H- or α-^{32}P-labeled dMTP); 0.024 mM $(dN)_n$ and oligomer $(dM)_m$ as indicated. This buffer system is designated MME. Some Pol I reactions were performed under these conditions. The enzyme concentrations were as indicated.

The reactions were started by addition of enzyme and were incubated at 37 or 25° as indicated. Acid precipitable radioactivity was determined as described (Nishimura et al., 1964) except that filters were pretreated with a solution of 50 mM potassium phosphate (pH 7.5), 50 mM pyrophosphate, 20 mM EDTA, and 5 mM rATP to lower background levels. V_0, initial velocity, was taken from multipoint linear kinetic plots over 6 min and is expressed as picomoles incorporated of nucleotide/milliliter of reaction per minute. The extent of reaction is expressed as picomoles incorporated/milliliter of reaction in 60 min. Reproducibility of the comparative assays was a function of the enzyme and of the template · primer involved. The limits of sensitivity of dMMP incorporation were 10 pmol of dMMP incorporated/ml per minute and the error in incorporation was ±3–10%. The variability due to template:· primer was due in some cases to the presence of more than one polymer · oligomer structure.

Physical Studies. Mixing curves were performed by combining solutions of oligo- and polynucleotides as varying concentrations into the appropriate buffer (as indicated) such that the total nucleotide concentration was constant. Absorbances were determined in a Zeiss PMQ II spectrophotometer connected for temperature control to a Lauda/Brinkmann K-2/R circulator. Temperature was measured with a thermistor in a cuvet containing a blank solution. The samples generally were mixed on ice and incubated at the specified temperature. For mixing and melting curves which were read at 5°, the samples were incubated for 5–60 min at 25° to ensure complex formation and then were kept at 5° overnight.

Theoretical mixing curves were calculated from the concentration and absorbance of each structure assumed to be present, using the extinction coefficients for single strand, duplex, and triplex polymer (Riley et al., 1966). Using the absorbance and concentration of triplex present in the 33 mol % $(dA)_{12}$ samples from the 5° mixing curve shown in Figure 2, the extinction coefficient at 260 nm of $(dA)_{12} \cdot 2(dT)_n$ was determined to be 5.7 A/mM. For comparison, the polymer extinction coefficient of $(dA)_n \cdot 2(dT)_n$ was 5.3 A/mM. Likewise, the extinction coefficient of $(rA)_{11} \cdot (dT)_n$ was determined from the 50 mol % $(rA)_{11}$ samples of the 5° mixing curve to be 6.4 A/mM at 260 nm. This was not significantly different from 6.5 A/mM for polymer duplex $(rA)_n \cdot (dT)_n$. The theoretical mixing curves were calculated using these oligomer extinction coefficients. In all cases, the theoretical curves (Results) were calculated assuming that only triplex or dublex was formed, independent of stoichiometry.

Extinction coefficients for absorbance at 285 nm were calculated from the concentrations determined at 260 nm and the absorbance at 285 nm. The extinction of duplex and triplex at 285 nm was calculated from the theoretical triplex and duplex concentrations in the 33 and 50 mol % $(dA)_{12}$ samples, respectively, and the experimentally determined absorbance at 285 nm.

Absorbance–temperature transitions were performed as previously described (Wells et al., 1970). Cuvets were equilibrated in the cell compartment at 10° before the samples were added, and the samples were equilibrated for at least 15 min before the temperature was raised. T_m values were reproducible within ±2°. At the conclusion of the melting curve, the temperature was decreased slowly; the cooling curves followed the melting transitions within 5° with some hysteresis.

The buffer systems used for mixing and melting curves were essentially those used in the comparative enzyme assays. TM buffer was 50 mM Tris-HCl (pH 8.1)–10 mM $MgCl_2$. MME buffer was 33 mM morpholinopropanesulfonate-KOH (pH 7.0)–13 mM $MgCl_2$–10% (v/v) ethanol.

Analytical buoyant density analyses in neutral Cs_2SO_4 solution were performed as described (Wells and Larson, 1972). Samples, 50 μM polymer and the appropriate amount of oligomer in a final volume of 0.150 ml of MME, were incubated at least 1 hr at 25° to ensure complex formation before saturated Cs_2SO_4 solution was added. Samples containing $(rA)_{23}$ and $(dA)_{23}$ were preincubated at 65° for 10 min before incubation at 25° to ensure complete complex formation.

Determination of Size of Polymerase Products. The size of the products formed by Pol III with $(rA)_{11}$ as primer was determined by analytical polyacrylamide gel electrophoresis (Burd and Wells, 1974). The reaction mixture used in the comparative assays was scaled up tenfold. Synthesis was allowed to proceed for 1 hr when incorporation of [α-^{32}P]dAMP had leveled off. The reaction was stopped by making the solution 0.03 M in EDTA and the mixture was applied to a Sephadex G50 column which was equilibrated with water. The sample was washed through the column with distilled water and the distribution of product and unreacted triphosphate was monitored by total and by Cl_3CCOOH-precipitable radioactivity. The triphosphates

Table I: Comparative Ability of Ribo- and Deoxyoligomers to Serve as Primers for *E. coli* DNA Polymerase I.[a]

Oligomer Concn (μM)	$(dC)_{10}$ or $(rC)_{10}$		$(dG)_{10}$ or $(rI)_{11}$		$(dT)_{10}$ or $(rU)_9$		$(dA)_{12}$ or $(rA)_{11}$	
	V_0[b]	Ext[b]	V_0	Ext	V_0	Ext	V_0	Ext
Deoxy 0	<10	12	1	170	20	1,100	0	<10
6	<10	80	1200	22,200	2600	23,100	<2	<10
12	<10	114	1600	25,300	2500	20,800	<2	<10
18	<10	131	1300	22,000	1800	20,800	<2	<10
24	<10	161	2200	28,900	1200	19,700	<2	<10
Ribo 6	<10	<20	430	15,700	20	1,100	532	3190
12	<10	<20	670	19,000	30	1,100	746	4810
18	<10	<20	700	20,400	20	800	854	5900
24	<10	<20	970	22,400	30	1,100	865	6940

[a] Experiments were performed as described under Materials and Methods. Reactions were at 25° except for the reactions with $(dG)_{10}$ and $(rI)_{11}$, which were at 37°. The specific activities (picomoles/milliliter per counts per minute) were: [^{3}H]-dCTP, 0.87; [^{3}H]dGTP, 0.65; [^{3}H]dTTP, 0.80; [α-^{32}P]dATP, 0.72. Pol I was at 1.0 μg/0.150 ml reaction volume. [b] V_0 is initial velocity, expressed as picomoles of mononucleotide incorporated/milliliter reaction volume per minute. Ext is extent of reaction, expressed as picomoles of mononucleotide incorporated/milliliter reaction volume in 60 min. Zero initial velocity means that no detectable synthesis above the no-enzyme blank was observed in the first 3 min of the reaction, although by 60 min some synthesis above background was observable. The limits of sensitivity of these reaction kinetics were 10 pmol/ml per min for V_0, and 30 pmol/ml per 60 min for Ext. Error was ±3%.

Table II: Comparative Ability of Ribo- and Deoxyoligomers to Serve as Primers for the *M. luteus* DNA Polymerase.[a]

Oligomer Concn (μM)	$(dC)_{10}$ or $(rC)_{10}$		$(dG)_{10}$ or $(rI)_{11}$		$(dT)_{10}$ or $(rU)_9$		$(dA)_{12}$ or $(rA)_{11}$	
	V_0[b]	Ext[b]	V_0	Ext	V_0	Ext	V_0	Ext
Deoxy 0	5	72	5	33	80	2,300	<10	24
6	37	1080	2070	22,500	2000	19,600	<10	43
12	44	1310	2730	25,700	1700	19,000	<10	38
18	52	1280	3100	28,800	1300	17,800	<10	37
24	60	1500	3330	30,800	900	16,300	<10	35
Ribo 6	11	362	1700	20,100	200	2,000	465	15,600
12	16	380	3130	28,400	60	2,000	610	17,300
18	26	436	3230	27,500	90	2,900	650	17,900
24	27	482	3830	35,400	80	3,100	678	17,300

[a] Experiments were performed as described in Materials and Methods in the legend to Table I, except that the *M. luteus* polymerase was used at 0.13 μg/0.150 ml reaction volume. [b] See legend to Table I.

were included; the product peak at the void volume was pooled. Half of the pool was made 0.3 *M* in KOH and was incubated 18 hr at 37° to hydrolyze the $(rA)_{11}$ primer. The base hydrolysate then was neutralized with Dowex 50-H^+. The concentrated pools of hydrolyzed and unhydrolyzed product were annealed with a slight excess of $(dA)_n$ for 10 min at 55° to release the product from the $(dT)_n$ which was still present. The samples were applied to 20% analytical gels (Burd and Wells, 1974). Parallel gels with appropriate markers, rAMP, $(dA)_2$, $(dA)_4$, and a pancreatic DNase digest of $(dA)_n$, were run as controls. After the run, the gels containing radioactivity were sliced into 0.3-cm slices and were counted by Cerenkov radiation. Total recovery of radioactivity from the reaction mixture to gel was 60–80% for the unhydrolyzed pools. For the alkali-treated pools, recovery ranged from 30 to 70%; the losses occurred during neutralization with Dowex 50-H^+ and during concentration due to nonspecific adsorption by Dowex and glass.

To determine the product size for $(rA)_{23}$ priming, essentially the same procedure was followed. Instead of neutralizing with Dowex 50-H^+, the hydrolyzed pools were passed through Bio-Gel P2 columns. Total recovery of radioactivity from reaction mixture to gel was 40% for both hydrolyzed and unhydrolyzed pools.

Paper Chromatography. Descending paper chromatography was performed on Whatman #1 paper in the following systems: system A, isobutyric acid–concentrated ammonia–water (66:1:33); system B, 0.1 *M* sodium phosphate (pH 6.8) (100 ml)–ammonium sulfate (60 g)–1-propanol (2 ml); system C, 1-propanol–concentrated ammonia–water (55:10:35); system D, 1 *M* ammonium acetate (pH 7.5)–95% ethanol (70:30).

Results

Comparative DNA Polymerase Assays. Assays to compare ribooligomers vs. deoxyoligomers as primers were performed with *E. coli* Pol I, *M. luteus* DNA polymerase, AMV DNA polymerase, and *E. coli* Pol III. A homodeoxyribopolymer combined with a complementary homooligomer was used as template · primer for the incorporation of the dMMP which was complementary to the template. Typical kinetics are shown in Figure 2 and the results are presented in Tables I to IV.

The results may be analyzed by three types of comparisons. First, the ability of individual oligomers to serve as primers for a given enzyme may be analyzed. Except with Pol III, $(dG)_{10}$ was the most efficient primer by the criteria of both initial rates and extent of reaction. Also, $(dT)_{10}$ was utilized efficiently by all four enzymes and $(rI)_{11}$ served efficiently for Pol I and the *M. luteus* polymerase. Notably,

Table III: Comparative Ability of Ribo- and Deoxyoligomers to Serve as Primers for the AMV DNA Polymerase.[a]

Oligomer Concn (μM)	$(dG)_{10}$ or $(rI)_{11}$		$(dT)_{10}$ or $(rU)_7$	
	V_0[b]	Ext[b]	V_0	Ext
Deoxy 0	<10	24	<2	60
0.1	<10	280	<2	122
0.5	24	621	<2	173
1.0	28	805	<2	165
30.0	38	1210	<2	141
Ribo 0.1	<2	24	<2	38
0.5	<2	61	<2	21
1.0	<2	66	<2	30
30.0	<2	93	<10	40

[a] Experiments were performed as described in Materials and Methods. Reactions were at 37°. The specific activities (pmol/ml per cpm) were: [^{3}H]dCTP, 0.047; [^{3}H]dGTP, 0.140; [^{3}H]dTTP, 0.036; and [^{3}H]dATP, 0.097. The AMV polymerase was used at 1.0 μg/0.150 ml reaction volume. Experiments also were performed with $(dC)_{10}$ or $(rC)_6$ and $(dA)_8$ or $(rA)_8$ as primers in their appropriate systems. No incorporation was found at any oligomer concentration up to 30 μM within the limits of the assay (<30 pmol incorporated/ml in 60 min). [b] See legend to Table I. Error was ±10%.

Table IV: Comparative Ability of Ribo- and Deoxyoligomers to Serve as Primers for *E. coli* DNA Polymerase III.[a]

Oligomer Concn (μM)	$(dT)_{10}$ or $(rU)_9$		$(dA)_{12}$ or $(rA)_{11}$	
	V_0[b]	Ext[b]	V_0	Ext
Deoxy 0	1	4	<2	<30
6	17	206	ND	ND
12	20	190	<2	<30
18	ND	ND	<2	<30
24	16	293	<2	<30
Ribo 6	<2	<10	120	3330
12	<2	<10	298	5290
18	ND	ND	ND	ND
24	<2	<10	282	4400

[a] Experiments were performed as described in Materials and Methods. Reactions were at 25°. The specific activities (pmol/ml per cpm) were: [^{3}H]dCTP, 1.04; [^{3}H]dGTP, 0.86; [^{3}H]dTTP, 0.63; and [α-^{32}P]dATP, 0.94. Pol III was used at 0.56 μg/0.150 ml reaction volume. Experiments also were performed with $(dC)_{10}$ or $(rC)_{10}$ and $(dG)_{10}$ or $(rI)_{11}$ as primers in their appropriate systems. No incorporation was found at any oligomer concentration up to 24 μM within the limits of the assay (<30 pmol incorporated/ml in 60 min). [b] See legend to Table I. Error was ±10%.

$(rA)_{11}$ was by far the most efficient primer for Pol III. Those oligomer combinations that did not prime significantly were as follows: for Pol I—$(rC)_{10}$ and $(dA)_{12}$; for *M. luteus* polymerase—$(dA)_{12}$ although it would prime limited synthesis with a very low initial rate; for the AMV enzyme—$(dC)_{10}$, $(rC)_6$, $(rI)_{11}$, $(rU)_7$, $(rA)_{11}$, and $(dA)_{12}$; for Pol III—$(dC)_{10}$, $(rC)_{10}$, $(dG)_{10}$, $(rI)_{11}$, $(rU)_9$, and $(dA)_{12}$.

Second, the capacity of deoxy- vs. ribooligomers to serve as primers may be compared. Except for $(dA)_m$, the deoxyoligomers primed better than the ribooligomers. The deoxyoligomers were 1- to 50-fold more active than the ribooligomers for all four polymerases (Tables I–IV). Only with the *M. luteus* DNA polymerase did $(rI)_{11}$ prime as efficiently as $(dG)_{10}$.

Third, the relative abilities of the different polymerases to utilize a given template · primer can be analyzed. Oligomers can serve satisfactorily as primers for all the DNA polymerases. Except for the Pol III and for the AMV enzyme, the polymerases displayed qualitatively similar preferences among oligomers. The AMV polymerase was unique in that it did not utilize any of the ribooligomers to prime DNA synthesis; prior studies (Wells et al., 1972) showed that polyribonucleotides could serve as primers. However, its preferences among the deoxyoligomers were similar to those of Pol I and the *M. luteus* polymerase. Also, Pol III was unique in that it used $(rA)_{11} \cdot (dT)_n$ markedly better than any other oligomer · polymer complex.

Two striking exceptions to these three general trends from the comparative assay results were the priming (1) by $(dT)_{10}$ and (2) by $(rA)_{11}$. (1) For all primers except $(dT)_{10}$, initial rate and extent of reaction generally increased with oligomer concentration (except for Pol III). This relationship, however, was not strictly linear with either rate or extent (Tables I–IV). In contrast, with $(dT)_{10}$, initial rates and extents leveled off or even decreased as the thymine/adenine ratio approached one. The decrease in rate and extent with increasing $(dT)_{10}$ concentration was especially evident with the *M. luteus* DNA polymerase and Pol I (Tables I and II). At least for Pol III, no dTMP incorporation was observed when the thymine to adenine ratio was 3.5 (results not shown). This inhibition was not due to contamination of the oligomer by a nonspecific inhibitory substance since no inhibition was found when the oligomer (at 24 μM) was added to an activated salmon sperm DNA primed reaction. Also, inhibition due to $(dT)_{10}$ bearing 3′-phosphoryl groups was not likely since pretreatment of the $(dT)_{10}$ with phosphatase before addition to the reaction mixture provided no enhancement of activity. Studies aimed at understanding the mechanism of the inhibition with $(dT)_{10}$ are described below.

(2) The marked preference for the ribo over the deoxy primer was unique to the adenylate oligomers among the primers tested. This case also was notable since $(dT)_n \cdot (rA)_m$ was the most efficient template · primer for Pol III (Table IV and Figure 2). Tables I–IV show that $(rA)_{11}$ was 260- to 500-fold more active than $(dA)_{12}$ especially at adenine/thymine ratios of ½ or ⅔, except for the AMV polymerase.

The uniqueness of the $(rA)_m$ priming ability compared to $(dA)_m$ could be due to: (1) $(dA)_m$ may be chemically abnormal; (2) $(dA)_m \cdot (dT)_n$ may form some structure not suitable for binding and/or elongation by polymerases in general; (3) the enzymes may have specificities for the presence or absence of a 2′-OH for some primers.

The chemical abnormality of $(dA)_{12}$ is unlikely for the following reasons. First, analysis of the $(dA)_{12}$ preparation by gel electrophoresis (Burd and Wells, 1974) showed that the molecule was predominantly the 12-mer plus oligomers $(dA)_{14}$, $(dA)_{16}$, and $(dA)_{18}$. Second, treatment of the $(dA)_{12}$ preparation with phosphatase did not increase its utilization under comparative assay conditions (results not shown). Third, different preparations of $(dA)_{12}$, both commercial and homemade, as well as dA's of different lengths, all proved to be less efficient primers than $(rA)_m$ under the same conditions. Finally, $(dA)_{12}$ combined with $(dT)_{11}$ efficiently primed the exponential synthesis of $(dA)_m \cdot (dT)_n$

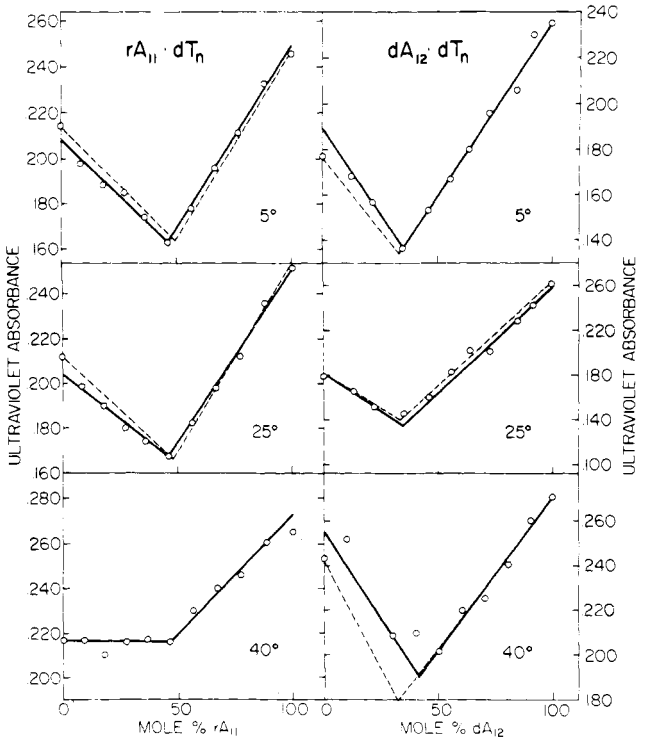

FIGURE 3: Mixing curves of $(dA)_{12}$ or $(rA)_{11}$ and $(dT)_n$ at three temperatures in MME buffer: (-O-) experimentally determined points; (- - -) theoretical mixing curves. The theoretical curves for the $(dA)_{12}$ complexes with $(dT)_n$ were calculated assuming only triplex formation was occurring and using the oligomer triplex extinction coefficient (5.7 A/mM) determined from the 5° curve. The theoretical curves for the $(rA)_{11}$ complexes with $(dT)_n$ were calculated assuming only duplex formation was occurring and using the polymer duplex extinction coefficient (6.5 A/mM) (Riley et al., 1966). The $(dA)_{12}$ mixtures were incubated at 5° for 12 hr before reading, at 25° for 2 hr, and at 40° for 15 min. Those mixtures read at 40° were allowed to incubate another 1.5 hr at 25° and were read again, which produced a curve similar to that shown at 25° with maximum hypochromicity at 33 mol % $(dA)_{12}$. Incubation of $(rA)_{11}$ was at 5° for 16 hr, at 25° for 2 hr, and at 40° for 15 min. All mixtures were mixed on ice; those mixtures to be incubated overnight at 5° were preincubated 5 min at 25° before cooling to 5° to assure complex formation. Incubation for longer times at 40° did not cause more or less hypochromicity, but did tend to increase the scatter of the points. The concentrations of 100% $(dA)_{12}$ and 100% $(dT)_n$ in the 5° curve were 28.0 and 21.0 μM; in the 25° curve they were 31.2 and 22.2 μM; in the 40° curve they were 32.3 and 30.0 μM, respectively. The concentrations of 100% $(rA)_{11}$ and 100% $(dT)_n$ in all three curves were 22.6 and 26.2 μM, respectively.

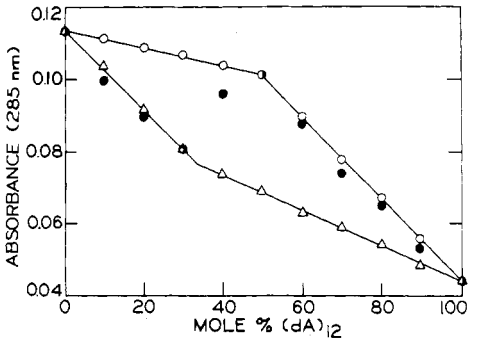

FIGURE 4: Mixing curve of $(dA)_{12}$ and $(dT)_n$ at 285 nm in MME buffer. The mixing curve was performed as described in Materials and Methods. The mixtures were read at 25° after incubating 5 min at 25°: (●) the experimentally determined points; (○) the theoretical duplex curve; (△) the theoretical triplex curve. The theoretical triplex curve at 285 nm was calculated assuming only triplex formation was occurring at all relative concentrations; the expected triplex concentration in the 33 mol % $(dA)_{12}$ sample and its absorbance at 285 nm were used for the calculation. The concentrations of 100% $(dA)_{12}$ and 100% $(dT)_n$ were 26.2 and 27.9 μM, respectively. Reproducibility was within pipetting error (±3%).

by Pol I in the presence of dATP and dTTP under published conditions (Byrd et al., 1965). Thus, the $(dA)_{12}$ was a suitable primer under some conditions.

To determine if $(dA)_m \cdot (dT)_n$ was forming a structure which could not be utilized by the polymerases, physical analyses of the adenine–thymine system were performed. In addition, the effect of the presence or absence of a 2′-OH and its interrelation with structural considerations is studied below.

Mixing Curves of $(dT)_n + (rA)_{11}$ *or* $(dA)_{12}$. Mixing experiments were performed under the conditions used in the comparative assays in order to determine the structures encountered by Pol III. Figure 3 shows that $(dA)_{12}$ formed predominantly triplex with $(dT)_n$, whereas $(rA)_{11}$ formed predominantly duplex in MME buffer. Mixing curves were performed at 5, 25, and 40° to determine if temperature would alter the stoichiometry of complex formation. At all three temperatures, triplex was the predominant complex of $(dT)_n$ with $(dA)_{12}$. However, at 40°, a leveling effect between 30 and 50 mol % was pronounced, and maximum hypochromicity occurred at approximately 50%. The change in maximum hypochromicity for the 25 and 40° plots was produced whether the temperature of the solutions was raised from 25 to 40° or was lowered from 40 to 25°. Thus, the shift indicated an equilibrium effect. The amount of hypochromicity at 25 and 40° was less than that found at 5°, indicating that less complex formation was occurring at the higher temperatures. Also, comparison of the data with the theoretical mixing curves substantiated that less complex was present at 40°. In this case, the theoretical duplex curve (not shown) would more closely approximate the experimental points than the triplex curve. Determinations also were performed at 285 nm. For $(rA)_{11} + (dT)_n$, the data were in excellent agreement (±2%) with the theoretical duplex mixing curve (not shown), indicating that the structure formed was independent of stoichiometry. Figure 4 shows that for $(dA)_{12}$, on the other hand, a triplex structure was formed below 50 mol % $(dA)_{12}$. This change in structure with stoichiometry and temperature showed that the interaction between $(dA)_{12}$ and $(dT)_n$ was not an all-or-none phenomenon.

Melting Curves on $(dT)_n + (dA)_{12}$ *or* $(rA)_{11}$. Melting curves are another method of structural analysis that could indicate the presence of different structures. Figure 5 shows melting curves of $(dA)_{12}$ complexes with $(dT)_n$ in MME at two wavelengths. $(dA)_{12} \cdot 2(dT)_n$ melted essentially in one phase with a slight depression prior to the major hyperchromic shift, as monitored at 260 nm. The major hyperchromic shift began slightly before the equivalent phase transition for $(dA)_{12} \cdot (dT)_n$. At 285 nm, a slight hyperchromism developed. The melting transitions were somewhat broad, presumably due to the short-chain oligomers in the presence of $MgCl_2$. These results, coupled with the correspondence of the 260- and 285-nm absorbances with the expected absorbances calculated from extinction coefficients for triplex and single strands for both wavelengths at both low (10°) and high (80°) temperatures, indicated that the observed transition was triplex to single strands.

$(dA)_{12} \cdot (dT)_n$ melted quite differently from $(dA)_{12} \cdot 2(dT)_n$, having a significant depression between 28 and 35° at 260 nm and a dramatic decrease in absorbance at 285 nm above 35°. This hypochromicity was due apparently to

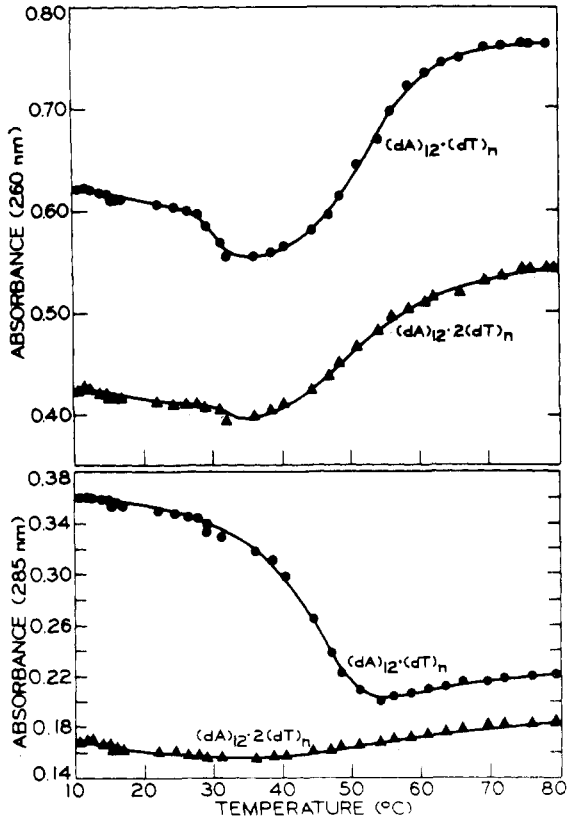

FIGURE 5: Melting curves of $(dA)_{12}$ and $(dT)_n$ complexes in MME buffer. Samples were prepared and equilibrated as described in Materials and Methods. The concentration of the $(dA)_{12} \cdot (dT)_n$ mixture was 48 μM $(dT)_n$ and 42 μM $(dA)_{12}$. The concentration of the $(dA)_{12} \cdot 2(dT)_n$ mixture was 48 μM $(dT)_n$ and 21 μM $(dA)_{12}$.

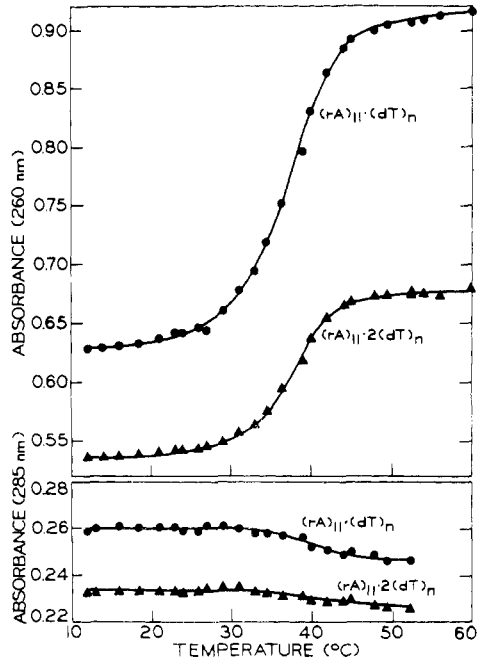

FIGURE 6: Melting curves of $(rA)_{11}$ and $(dT)_n$ complexes in MME buffer. The solutions were prepared as described in Materials and Methods. The concentrations of $(rA)_{11}$ were 24 and 48 μM and the concentration of $(dT)_n$ was 48 μM.

a duplex to triplex transition: $2[(dA)_{12} \cdot (dT)_n] \rightarrow (dA)_{12} \cdot 2(dT)_n + (dA)_{12}$. Except for this difference, the pattern for $(dA)_{12} \cdot (dT)_n$ was that expected for a triplex to single-strand transition as seen with $(dA)_{12} \cdot 2(dT)_n$ (the T_m for both was 51°).

Figure 6 shows that the melting curves for $(rA)_{11} \cdot (dT)_n$ and $(rA)_{11} \cdot 2(dT)_n$ were quite different from the $(dA)_{12}$ complexes, but were very similar to each other in shape, width, and T_m (38°). The absorbance at 260 and 285 nm corresponded to that expected for a duplex to single-strand transition in both cases. The transition at 285 nm was slightly hypochromic, as expected for a duplex to single-strand transition.

Buoyant Density Analyses on $(dT)_n + (rA)_{11}$ or $(dA)_{12}$. The results of buoant density analyses of the complexes with $(dT)_n$ are shown in Table V and Figure 7. $(dA)_{12} \cdot (dT)_n$ and $(dA)_{12} \cdot 2(dT)_n$ formed complexes of approximately the density of the polymer triplex. Free $(dA)_{12}$ was not observed in the $(dA)_{12} \cdot (dT)_n$ determination presumably because of its low molecular weight. $(rA)_{11}$, on the other hand, formed two complexes at a 1/1 ratio with $(dT)_n$, one approximately equal to the expected duplex density and the other slightly lighter than the expected triplex density. $(rA)_{11} \cdot 2(dT)_n$ produced a complex which was somewhat less dense than the expected triplex but substantially more dense than duplex. The lighter densities of the oligomer complexes compared to the polymer · polymer complexes could be due to the presence of single-stranded $(dT)_n$ tails, to single-stranded regions in the complex, or to the irreversible diffusion of oligomer from the complex.

To summarize the density results, $(dA)_{12} + (dT)_n$ formed triplex structures preferably to duplex at all adenine/thymine ratios. Alternatively, $(rA)_{11}$ formed a mixture of duplex and triplex at a ratio of one and predominantly triplex at a 1/2 ratio. The high salt used in the buoyant density analyses would be expected to enhance triplex formation compared to the enzymatic reaction conditions.

Table V: Analytical Buoyant Densities of Complexes of $(dT)_n$ with $(rA)_m$ or $(dA)_m$.

Nucleic Acid	Density (g/ml) Values[a] Where $m = n$	Experimental $m = 11, 12$	Experimental $m = 23$
$(rA)_m \cdot (dT)_n$	1.433	1.505, 1.440	1.444
$(rA)_m \cdot 2(dT)_n$	1.519	1.497	1.508
$(dA)_m \cdot (dT)_n$	1.419	1.488	1.473
$(dA)_m \cdot 2(dT)_n$	1.492	1.484	1.489
$(dT)_n$	1.428	—	—
$(dA)_n$	1.379	—	—
$(rA)_n$	1.570	—	—

[a] Taken from Riley et al. (1966); Wells et al. (1970), and Wells and Larson (1972); a dash means not applicable.

Effect of Temperature on Ability of $(dA)_{12}$ to Serve as Primer. Figure 3 suggested that the $(dA)_{12} \cdot 2(dT)_n$ complex underwent a modest triplex to duplex transition with increasing temperature. Thus, studies were performed to determine if this slight shift to more duplex structure might increase the priming efficiency of that mixture. Using Pol I, the stimulation of synthesis by temperature was tested on $(rA)_{11} \cdot (dT)_n$, $(dA)_{12} \cdot (dT)_n$, $(dA)_{12} \cdot 2(dT)_n$, and $(dA\text{-}dT)_n \cdot (dA\text{-}dT)_n$ as a control (Figure 8). The stimulation with increasing temperature was marked for $(rA)_{11} \cdot (dT)_n$ up to 25°, was almost linear for $(dA\text{-}dT)_n \cdot (dA\text{-}dT)_n$, and was very low with $(dA)_{12} \cdot (dT)_n$ and $(dA)_{12} \cdot 2(dT)_n$. The substantial stimulation with $(rA)_{11} \cdot (dT)_n$ and $(dA\text{-}dT)_n \cdot (dA\text{-}dT)_n$ represented both kinetic stimulation of the en-

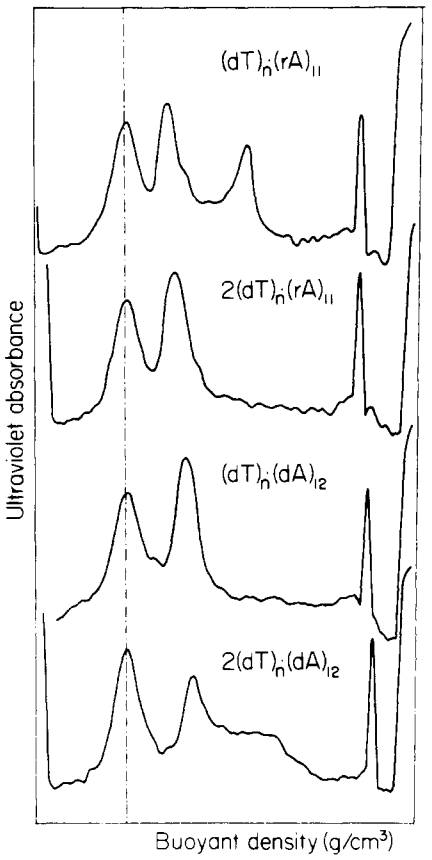

FIGURE 7: Analytical buoyant density analyses of $(rA)_{11}$ and $(dA)_{12}$ complexes with $(dT)_n$ in neutral Cs_2SO_4 solution. The buoyant density analyses were performed as described in Materials and Methods. The dotted line indicates the position of the $(dA\text{-}dBU)_n \cdot (dA\text{-}dBU)_n$ reference standard ($\rho = 1.538$ g/ml); the peaks on the extreme right are the miniscus.

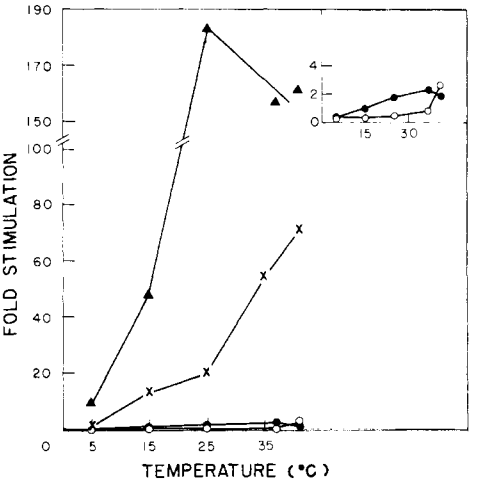

FIGURE 8: Effect of temperature on $(dA)_{12}$ and $(rA)_{11}$ priming with Pol I. The assays were performed in MME buffer as described in Materials and Methods except that identical reaction mixtures were incubated at 5, 15, 25, 37, and 41°. Synthesis using 26 μM $(dA\text{-}dT)_n \cdot (dA\text{-}dT)_n$, with 0.120 m$M$ dTTP present as well as dATP, was used as a control. The $(dT)_n$ concentration was 27 μM. Pol I was used at 3 μg/0.150 ml reaction volume. Fold stimulation is the ratio of V_0 at the given temperature to the V_0 of $(dA\text{-}dT)_n \cdot (dA\text{-}dT)_n$ synthesis at 5°. V_0 is expressed as picomoles/milliliter per minute, and onefold synthesis is 13 pmol/ml per min: (○) $(dA)_{12} \cdot 2(dT)_n$; (●) $(dA)_{12} \cdot (dT)_n$; (▲) $(rA)_{11} \cdot (dT)_n$; (X) $(dA\text{-}dT)_n \cdot (dA\text{-}dT)_n$; Axes for the inset are the same as for the figure.

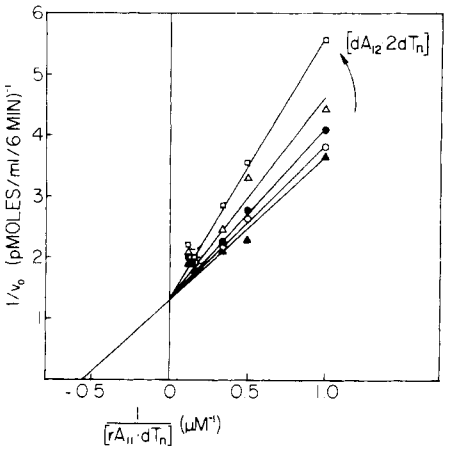

FIGURE 9: Kinetic analysis of inhibition of $(rA)_{11} \cdot (dT)_n$ by $(dA)_{12} \cdot 2(dT)_n$. The experiments were performed in MME buffer with Pol III as described in Materials and Methods, except that the concentrations of $(rA)_{11} \cdot (dT)_n$ and $(dA)_{12} \cdot 2(dT)_n$ were varied relative to each other. The $(rA)_{11} \cdot (dT)_n$ concentrations were 1, 2, 3, 6, and 8 μM nucleotide of $(rA)_{11}$. For all cases, the relative molar concentrations of nucleotide $(rA)_{11}$ to $(dT)_n$ were 1 to 2. The $(dA)_{12} \cdot 2(dT)_n$ concentrations were: (▲) 0; (○) 0.3; (●) 0.6; (△) 1.0; and (□) 2.0 μM nucleotide of $(dA)_{12}$.

zyme as well as slipping effects of template · primer chains. $(dA)_{12}$ and $(dT)_n$ at a 1/1 ratio were stimulated slightly more than the 1/2 mixture (inset in Figure 8), which suggested that more usable primers existed with $(dA)_{12} \cdot (dT)_n$. That very little stimulation was seen with $(dA)_{12} \cdot (dT)_n$ indicated that very little duplex or other usable template·primer structures were formed as the temperature increased.

Thus, $(dA)_{12} + (dT)_n$ forms a predominantly functional triplex, although slight structural changes occur with changes in stoichiometry and temperature. These changes are not quantitative conversions from or to a duplex structure, but, more likely, are minor shifts in relative concentrations of triplex and either duplex or intermediate structures.

Ability of $(dA)_{12} \cdot 2(dT)_n$ to Inhibit $(rA)_{11} \cdot (dT)_n$ Primed Synthesis. Figure 9 shows the ability of $(dA)_{12} \cdot 2(dT)_n$ to inhibit synthesis primed by $(rA)_{11} \cdot (dT)_n$. The variable substrate was $(rA)_{11} \cdot (dT)_n$ at a mole nucleotide ratio of 1/2, which was a combination that provided for maximum utilization of primer. dATP and Mg^{2+} were saturating and held constant. The triplex inhibitor, $(dA)_{12} \cdot 2(dT)_n$, was varied at different concentrations of $(rA)_{11} \cdot (dT)_n$. Initial rates were measured and expressed in a Lineweaver–Burke plot. The line for zero inhibitor concentration was extrapolated to give a K_m of 2.9 μM nucleotide $(rA)_{11}$ (average for three determinations).

At high concentrations of $(rA)_{11} \cdot (dT)_n$, substrate inhibition occurred, as indicated by the upward curve in the kinetic plot. This inhibition may represent the "gap specificity" attributed to Pol III (Kornberg and Gefter, 1972; Otto et al., 1973). The structures causing substrate inhibition may not necessarily have been triplex, but could have been duplexes where the $(rA)_{11}$ was not adjacent to a satisfactory gap. Since stoichiometry and stability of complex formation with oligomers are concentration dependent, increasing the $(rA)_{11}$ and $(dT)_n$ concentrations would increase the amount of $(rA)_{11}$ proportionately bound to $(dT)_n$. Hence, at higher concentrations, there may have been fewer or smaller gaps. Since Pol III has an associated single-strand specific nuclease, the presence of some single-strand $(dT)_n$

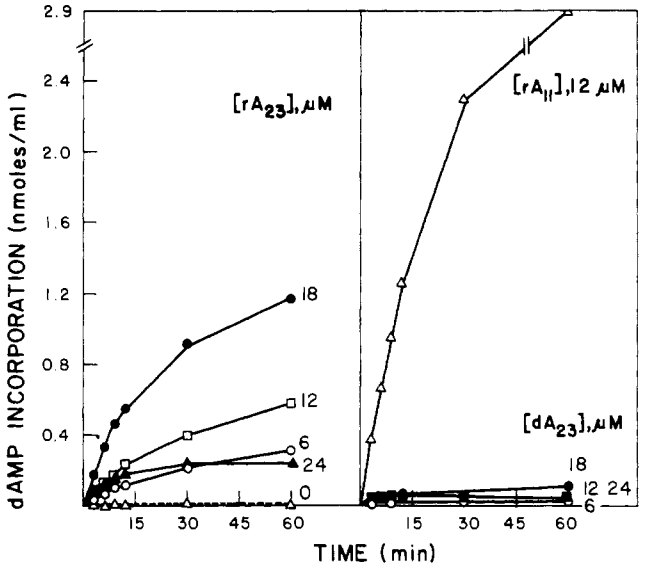

FIGURE 10: Ability of $(rA)_{23}$ and $(dA)_{23}$ to prime $(dT)_n$-templated synthesis with Pol III in MME buffer. The assays were performed as described in Materials and Methods. Reaction mixtures were preincubated for 10 min at 65° to ensure complex formation and cooled to 25° before enzyme was added; 0.56 μg of Pol III per 0.150 ml reaction volume was used. The $(dT)_n$ concentration was 24 μM.

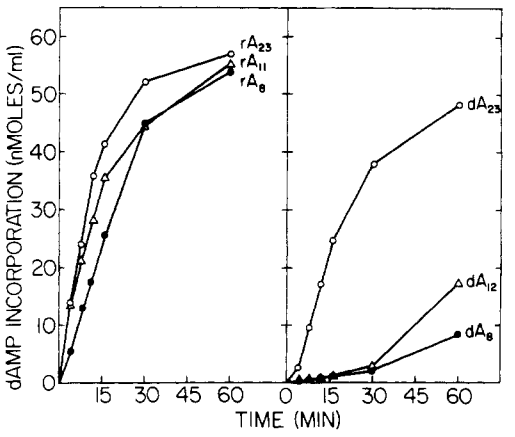

FIGURE 11: Priming by $(dA)_m$ and $(rA)_m$ with the *M. luteus* polymerase in TM buffer. Assays were performed as described in Materials and Methods. The reaction mixtures containing $(dA)_{23}$ or $(rA)_{23}$ were preincubated 10 min at 65° and cooled to 37° before enzyme was added. The $(dT)_n$ concentration was 24 μM and the oligomers were at 12 μM. *M. luteus* polymerase was used at 0.21 μg per 0.150 ml reaction volume. The reaction temperature was 37°.

could sequester the enzyme, which would be another source of the substrate inhibition seen.

When $(dA)_{12} \cdot 2(dT)_n$ was present, it caused inhibition of both initial rates and extents. The inhibition was competitive, and a replot (not shown) of the slopes from Figure 9 vs. triplex concentration produced a K_i of 2.2 μM nucleotide $(dA)_{12}$. When the K_i and K_m were divided by oligomer length to represent the concentration of the 3′-hydroxyl ends, the K_i and K_m became essentially equivalent (within experimental variation). The conclusion is that Pol III bound to the triplex but did not elongate it.

Size of Products of Pol III Reaction. To understand the above described kinetic results, size analyses were performed on products of Pol III reactions. These determinations were useful for establishing if the initial velocities were initiation or elongation rates and also for establishing the extent of utilization of $(rA)_{11}$. Analytical polyacrylamide gel analyses (Burd and Wells, 1974) were performed on the products of $(rA)_{11}$-primed reactions by Pol III in MME (see Materials and Methods). This technique could resolve individual oligomers from 1 to ~30 long. The R_f values of the radioactive products before and after alkaline hydrolysis were correlated with the R_f values of markers of known size. The product for $(rA)_{11}$ priming was predominantly $(dA)_9$, with product distribution ranging from the 7- to the 20-mer (data not shown). This sized product was formed independently of oligomer · primer concentration from 6 to 27 μM. Thus, if the oligomer concentration has an influence on gap size, it was not reflected in the product size. The size of the $(rA)_{11}$-primed reaction was further confirmed by nucleoside/nucleotide ratio, determined by venom phosphodiesterase degradation of [^{3}H]dAMP labeled DNA (M. J. Ryan, personal communication). These results are consistent with prior studies (Kornberg and Gefter, 1972) which showed that the product of $(dT)_{10} \cdot (dA)_n$ primed reaction was $(dT)_{10}$-$(dT)_{12}$.

With a knowledge of product size, an estimate of the extent of primer utilization could be calculated to determine the ability of the polymerase to recycle. Kornberg and Gefter estimated the purity of their enzyme at approximately 33% and the molecular weight at 140,000. Since our concentration of protein was 28 μg/ml, using 20 μl per 0.150 ml of reaction meant that 0.013 pmol of enzyme was present. For 0.012 mM $(rA)_{11}$, 0.16 nmol of ends was available per reaction. For 3 nmol/ml of reaction product formed, 0.05 nmol of ends were used, or 31% of the available ends. If each polymerase molecule was viable, based on the above assumptions there was 3.8×10^3 usable ends/enzyme. Thus, the enzyme was recycling, making short product chains. Hence, classical Michaelis–Menten kinetic analysis would produce kinetic parameters more representative of initiation rates than elongation rates.

Effect of Primer Chain Length. To clarify the distinction between triplex and duplex priming, the formation of a $(dA)_{12} \cdot (dT)_n$ duplex would have been an important control. However, efforts to form this duplex under conditions acceptable for Pol III activity were unsuccessful. Other workers (Cassani and Bollum, 1969) reported that in the absence of $MgCl_2$, longer (dA) oligomers formed duplexes in contrast to shorter oligomers which formed triplexes. Under our conditions (MME), the longer oligomers might form a higher proportion of duplex which would be reflected in greater priming capacity of the mixture.

The ability of the long oligomers to prime with Pol III was determined (Figure 10). $(rA)_{23}$ served as an efficient primer but was only approximately half as efficient as $(rA)_{11}$ (Figure 2) as expected from the number of 3′-hydroxyl ends present. Some synthesis was seen with $(dA)_{23}$, although none had been seen with $(dA)_{12}$ (Figure 2). The size of the product of the $(rA)_{23}$ primed reaction was analyzed as described above. The predominant product was $(dA)_8$ (results not shown), and was independent of $(rA)_{23}$ concentration (from 6 to 18 μM) as described above for $(rA)_{11}$. This indicated that the product length did not vary significantly with oligomer length or with oligomer concentration (effective gap size?) and thus suggests that the size is governed by the Pol III molecule.

The effect of oligomer length on priming with the *M. luteus* DNA polymerase was determined also (Figure 11). $(rA)_8$, $(rA)_{11}$, and $(rA)_{23}$ were compared with $(dA)_8$,

$(dA)_{12}$, and $(dA)_{23}$ at adenine to thymine ratios of 1/1 and 1/2. Initial rates and extents of reaction increased with oligomer length for both the ribo- and deoxyoligomers, but the increase with $(dA)_{23}$ was marked for the *M. luteus* polymerase. Similar results were found with Pol I (results not shown).

Physical Studies on $(dT)_n$ + $(dA)_{23}$ or $(rA)_{23}$. The better utilization of the longer oligomer by the polymerases could have been due to the presence of a greater proportion of duplex structures or to the greater stability of the nucleic acid complexes. To clarify these two possibilities, mixing curves, melting curves, and buoyant density analyses were performed.

Mixing curves (results not shown) were performed in MME buffer on mixtures of $(dT)_n$ with either $(rA)_{23}$ or $(dA)_{23}$. The results were very similar to those found for the shorter oligomers (Figure 3). $(rA)_{23}$ produced the expected duplex curves at 5, 25, and 40° with measurements at 260 and 285 nm. $(dA)_{23}$, however, produced maximum hypochromicity at 44 mol % $(dA)_{23}$ and the mixing curve at 285 nm was biphasic as in Figure 4 for $(dA)_{12}$, suggesting a dependence of structure on stoichiometry.

The melting curves for the longer oligomers also were similar to those seen with the short oligomers. $(rA)_{23}$ + $(dT)_n$ melted in one phase with a T_m of 48° for both 1/1 and 1/2 mixtures (data not shown). However, $(dA)_{23}$ formed a more stable complex than $(dA)_{12}$ with $(dT)_n$; the T_m of the $(dA)_{23} \cdot (dT)_n$ complexes was above 70°, and the transition was obscured by the boiling of the ethanol. A hypochromic shift from 30 to 60° at both 260 and 285 nm occurred with $(dA)_{23} \cdot (dT)_n$, as seen with $(dA)_{12} \cdot (dT)_n$ (Figure 5), but at higher temperatures than found for the $(dA)_{12}$ case. Thus, the longer oligomers had similar helix–coil transitions to the shorter oligomers, but displaced to higher temperatures; hence more duplex would be present at reacton temperatures.

Analytical buoyant density analyses in Cs_2SO_4 solution were performed to compare with the shorter oligomer complexes and to determine the tendency of $(dA)_{23}$ to form triplex or duplex in high ionic strength (Table V). $(rA)_{23} \cdot (dT)_n$ formed a complex of similar density to $(rA)_{11} \cdot (dT)_n$, which was slightly more dense than the expected duplex density for $(rA)_n \cdot (dT)_n$. $(rA)_{23} \cdot 2(dT)_n$ formed an apparent three-stranded complex of density intermediate between $(rA)_{11} \cdot 2(dT)_n$ and $(rA)_n \cdot 2(dT)_n$. On the other hand, $(dA)_{23} \cdot (dT)_n$ had a density 15 mg/ml lighter than $(dA)_{12} \cdot (dT)_n$, and 19 mg/ml lighter than $(dA)_n \cdot 2(dT)_n$. $(dA)_{23} \cdot 2(dT)_n$ was only 3 mg/ml lighter than $(dA)_n \cdot 2(dT)_n$. In summary, $(dA)_{12} \cdot (dT)_n$, $(dA)_{12} \cdot 2(dT)_n$, and $(dA)_{23} \cdot 2(dT)_n$ were forming the same complex, i.e., triplex, but $(dA)_{23} \cdot (dT)_n$ was forming a structure significantly less dense.

The effect of temperature (5–41°) on priming by $(dA)_{23}$ and $(rA)_{23}$ was determined also (data not shown). The adenine/thymine ratio had a greater effect on fold synthesis for $(dA)_{23}$ than for $(dA)_{12}$ (Figure 8). Whereas $(dA)_{12} \cdot (dT)_n$ was twofold better than $(dA)_{12} \cdot 2(dT)_n$ at 37°, $(dA)_{23} \cdot (dT)_n$ was fivefold better than $(dA)_{23} \cdot 2(dT)_n$. These results indicate that $(dA)_{23} \cdot (dT)_n$ was forming more usable structures than $(dA)_{12} \cdot (dT)_n$. These data combined with the physical studies indicate that these $(dA)_{23} \cdot (dT)_n$ structures were intermediate between triplex and duplex, probably a composite of both.

Role of Structure in Priming by $(dT)_{10}$. The ability of $(rA)_m$ to prime better than $(dA)_m$ was one of the anomalies of the comparative assay results. The other anomaly was the inhibition of priming observed when the $(dT)_{10}$ concentration was equal to the $(dA)_n$ concentration. Thus, studies were performed on $(dT)_{10} \cdot (dA)_n$ complexes to determine if polymer · oligomer structure played a role in this inhibition of priming.

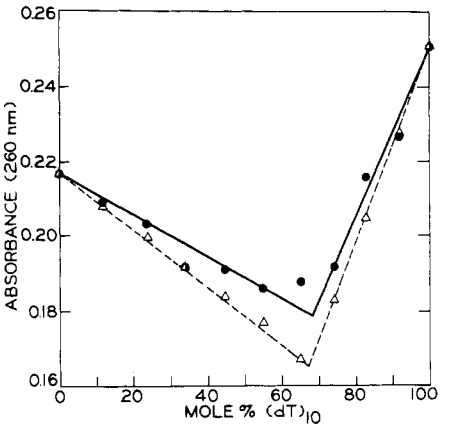

FIGURE 12: Mixing curve of $(dT)_{10}$ and $(dA)_n$ in TM buffer. Solutions were incubated 10 min at 65° and then 1 hr at 25° before reading at 25°. The 100 mol % $(dT)_{10}$ and 100 mol % $(dA)_n$ were 28.7 and 25.9 μM, respectively: (●) experimental points; (△) the theoretical triplex curve. The theoretical triplex curve was calculated with the oligomer triplex extinction coefficient of $(dA)_{12} \cdot 2(dT)_n$.

In TM buffer, priming was inhibited by $(dT)_{10}/(dA)_n$ ratios of 1/2 and higher (Tables I and II). Figure 12 shows that, at 25°, the mixing curve of $(dT)_{10}$ and $(dA)_n$ had a leveling of slope between 50 to 70 mol % $(dT)_{10}$, with maximum hypochromicity at approximately 50% suggesting that more than one structure was present. The experimental points correlated with the theoretical triplex curve, which indicated that triplex was probably the structure present in the high mole percent $(dT)_{10}$ samples. Also, melting studies on $(dT)_{10} \cdot (dA)_n$ and $2(dT)_{10} \cdot (dA)_n$ in TM buffer showed that both complexes had a major transition at 38°, but that the $(dT)_{10} \cdot (dA)_n$ mixture underwent a hyperchromic shift (11–30°) before it began the major transition. In summary, the $2(dT)_{10} \cdot (dA)_n$ mixture appeared to have one structure, which was probably triplex; the $(dT)_{10} \cdot (dA)_n$ mixture probably had more than just triplex structures present.

In MME buffer, inhibition of priming by $(dT)_{10}$ was seen at thymine/adenine ratios of one or more (Table IV). Mixing studies under reaction conditions showed that predominantly duplex, $(dT)_{10} \cdot (dA)_n$, existed. Also, the melting transitions of $(dT)_{10} \cdot (dA)_n$ and $2(dT)_{10} \cdot (dA)_n$ have the same width and T_m (45°) in this buffer (results not shown). Thus, the same structure, duplex, probably is present in both mixtures.

To further investigate the types of structures formed by $(dT)_{10}$ and $(dA)_n$, buoyant density analyses of $(dA)_n$, titrated with three concentrations of $(dT)_{10}$, were performed (Figure 13). The $(dT)_{10} \cdot 2(dA)_n$ mixture formed a complex which had approximately the density (3 mg/ml lighter) of the polymer duplex, $(dT)_n \cdot (dA)_n$ (1.419 g/ml). When the thymine/adenine ratio was increased to 1/1 and 2/1, the complexes formed were 7 and 9 mg/ml more dense, respectively, than polymer duplex, but much too light to be considered triplex. Since the third strand, in a Hoogsteen pairing configuration, is a short oligomer in this case, the triplex might be somewhat unstable due to the diffusion of the oligomer third strand away from the complex.

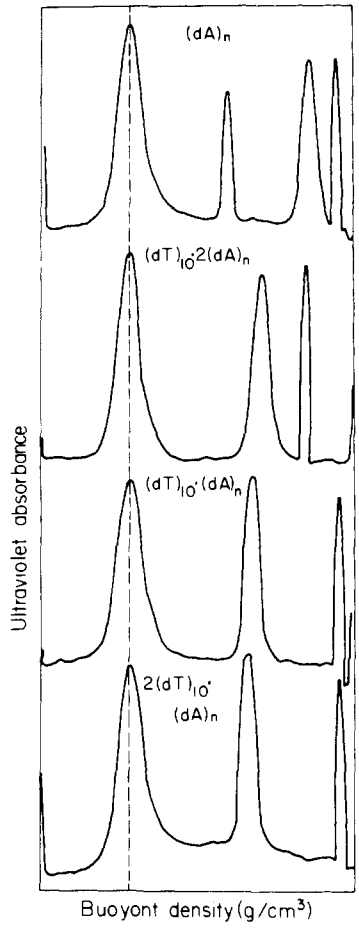

FIGURE 13: Analytical buoyant density analyses of $(dA)_n$ with three concentrations of $(dT)_{10}$. The samples were prepared as described in Materials and Methods. The buffer was MME and preincubation was for 2 hr at 25° before the Cs_2SO_4 solution was added. The solutions contained 7 nmol of $(dA)_n$ and 0, 3.5, 7, and 14 nmol of $(dT)_{10}$; the density values were 1.372, 1.416, 1.426, and 1.428 g/ml, respectively. The samples containing only $(dA)_n$ contained two internal standards, $(dA\text{-}dBU)_n \cdot (dA\text{-}dBU)_n$ (ρ = 1.538 g/ml) and T_4 DNA (ρ = 1.444 g/ml).

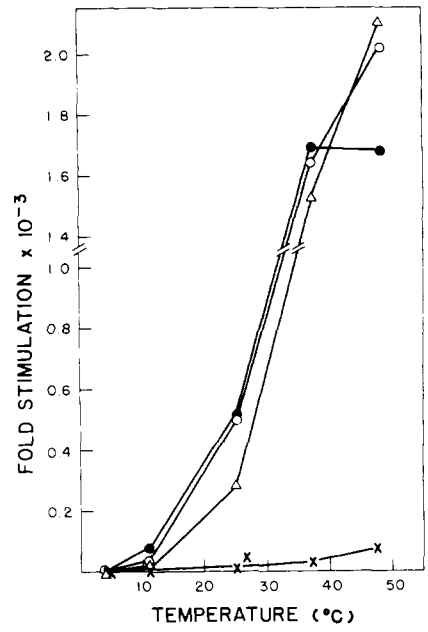

FIGURE 14: Effect of temperature on priming by $(dT)_{10}$ with $(dA)_n$ with the *M. luteus* DNA polymerase. The assays were performed in TM buffer as described for the *M. luteus* polymerase in Materials and Methods except the reaction mixtures were incubated at 5, 11, 25, 37, and 48°. Synthesis using 24 μM $(dA\text{-}dT)_n \cdot (dA\text{-}dT)_n$, with 0.120 m$M$ dATP present as well as dTTP, was used as a control; 0.13 μg per 0.150 ml reaction volume of *M. luteus* polymerase was used. Fold stimulation was determined as before (Figure 8) and onefold synthesis was 4 pmol/ml per min. The $(dA)_n$ concentration was constant at 24 μM: (X) $(dA\text{-}dT)_n \cdot (dA\text{-}dT)_n$; (△) $2(dT)_{10} \cdot (dA)_n$; (○) $(dT)_{10} \cdot (dA)_n$; (●) $(dT)_{10} \cdot 2(dA)_n$.

Since this is essentially irreversible, a triplex might become more duplex-like with time, resulting in the observed intermediate density. In summary, as the $(dT)_{10}/(dA)_n$ ratio approached and surpassed one, the polymer · oligomer structures formed were not classical duplexes. It was likely that at high ratios composite structures were formed which consisted of triplex, duplex, and even some single-stranded $(dA)_n$, all in one molecule.

The structural changes which these complexes appeared to undergo from the melting curves might be reflected in their priming ability at different temperatures. Figure 14 shows the effect of temperature on priming with the *M. luteus* polymerase in TM buffer. Unlike the $(dA)_{12} \cdot (dT)_n$ mixtures with Pol I, where increasing temperature produced very little stimulation (Figure 8), the $(dT)_{10}$ complexes stimulated many fold more than $(dA\text{-}dT)_n \cdot (dA\text{-}dT)_n$ by increasing temperature. The amount of stimulation at lower temperatures varied with thymine/adenine ratios. The $(dT)_{12} + 2(dA)_n$ mixture stimulated 50-fold more than the $(dT)_{10} + (dA)_n$ mixture at 11°, but was only 10-fold more at 25°. The $(dT)_{10} + (dA)_n$ mixture stimulated 10-fold more than the $2(dT)_{10} + (dA)_n$ mixture at 11°, but simulated 210-fold more at 25°. This was consistent with the $2(dT)_{10} \cdot (dA)_n$ mixture being mainly a triplex structure. Despite the lower oligomer concentration, more primer structures were available in the $(dT)_{10} \cdot 2(dA)_n$ mixture at 25°, and the amount of usable primer structures decreased with increasing relative $(dT)_{10}$ concentrations.

Discussion

Nucleic Acid Structure and Priming Ability. In a comparative study of polymerase activities, there are two approaches: either to maintain the same environment for all polymerases to minimize structural effects in the nucleic acids, or to use conditions that maximize enzyme activity and then define the substrate effects. In the first case, any differences in activity among the polymerases would be due solely to enzyme effects. This was the approach used with Pol I and the *M. luteus* polymerase. However, the low level of activity observable with Pol III required taking the second approach. Optimizing conditions for Pol III were required to increase the sensitivity of the assay, but changing the reaction conditions affected the template · primer structure.

The results of the comparative studies with the four DNA polymerases showed that generally deoxyribooligo primers were more, or as, effective as ribooligo primers. One striking exception to this generalization was that $(rA)_m$ was substantially more efficient than $(dA)_m$; this effect was more pronounced in MME buffer with Pol III. Three types of physical determinations (discussed below) indicated that $(dA)_{12} + (dT)_n$ had a propensity to form three-stranded complexes, which apparently could not serve as template · primers, whereas $(rA)_{11} + (dT)_n$ preferred to form conventional duplexes. The reason for this behavior is unknown. Competition experiments demonstrated that Pol III bound to the $(dA)_{12} \cdot 2(dT)_n$ triplex essentially as well as to

$(rA)_{11} \cdot (dT)_n$, but was not able to elongate the triplex primers. Previous studies (Riley et al., 1966; Morgan and Wells, 1968; Murray and Morgan, 1973) showed that nonduplex structures affected nucleic acid polymerase activities.

To further evaluate the relative role of the sugar moiety (ribo or deoxy) vs. nucleic acid structural influences, priming studies were performed with the longer oligomers $(rA)_{23}$ and $(dA)_{23}$. $(dA)_{23}$ was a substantially better primer than $(dA)_{12}$ and was essentially as efficient as $(rA)_{23}$ for the *M. luteus* DNA polymerase. Also, physical determinations showed that the longer dA oligomers tended to form more duplex-like structure with $(dT)_n$ than the shorter dA oligomers. Thus, the type of nucleic acid structure (duplex or triplex) which is present is of greatest importance for priming activity; the presence or absence of a 2'-OH is important since structure is influenced by this variable but is only of secondary importance per se since $(dA)_{23}$ and $(rA)_{23}$ are both effective primers.

Since the structures in the adenine–thymine system were complex and susceptible to changes in temperature and environmental conditions, it is certain that a detailed analysis of the guanine–cytosine system would also reveal structural anomalies. Non-Watson–Crick structures also were found for the G-C series (Michelson et al., 1967; Felsenfeld and Miles, 1967). Such anomalies may explain the low priming capacity of some of the cytosine oligomers.

The reverse transcriptase from AMV, like the other three DNA polymerases, prefers deoxy primers to ribo primers. This is consistent with past studies (Green and Gerard, 1974) which indicated that the reverse transcriptases were mechanistically similar to the well-characterized bacterial enzymes, including a general preference for deoxy templates except for certain cases. Hence, although specific RNA primers are utilized for initiation of provirus synthesis by the RNA tumor virus polymerase, it is apparent that this specificity does not reside in the polymerase but may be due to compartmentalization of the RNA primer with the polymerase.

In light of our results, some studies with oligomer · primers may be reevaluated. The purification and properties of a factor (factor II) which specifically stimulated Pol III on ϕX174 DNA · RNA hybrid and on $(dT)_{10} \cdot (dA)_n$ at a 3.5/1 ratio were described (Hurwitz and Wickner, 1974). The inability of Pol III to utilize $(dT)_m$ as primer with $(dA)_n$ at this high T/A ratio may be due to formation of triplex structures. Using the assay conditions specified in that study and the conditions described herein (see Materials and Methods) the activity of Pol III was determined on a variety of $(dT)_{10}/(dA)_n$ ratios, including 1/2 and 3.5/1. Under both sets of conditions, ratios less than one supported synthesis but a ratio of 3.5 supported essentially none (results not shown). Thus, factor II may be potentially interesting for its ability to convert inactive triplex to usable template · primer as well as for its interaction with and stabilization of Pol III.

Also, mammalian DNA polymerases were found to prefer $(dA)_m$ to $(rA)_m$ with $(dT)_n$, and to prefer $(dT)_m$ to $(rU)_m$ with $(dA)_n$ (Chang and Bollum, 1972). Our results also showed $(dT)_m$ to be a superior primer to $(rU)_m$. However, we found $(rA)_m$ to be preferred over $(dA)_m$; the reason for this apparent discrepancy is probably due to differences in reaction conditions. Chang and Bollum performed reactions at 35°. Under our reaction conditions, $(rA)_{11} \cdot (dT)_n$ would be partially melted at 35° but $(dA)_{12} \cdot (dT)_n$ is more stable than $(rA)_{11} \cdot (dT)_n$. Since Chang and Bollum performed studies in lower buffer concentrations, lower divalent metal ion concentration, and lower oligomer concentration (all destabilizing factors), it is probable that the $(rA)_m \cdot (dT)_n$ was at least partially melted, thus explaining the apparent discrepancy.

Nucleic Acid Structural Transitions. The structures of the oligomer · polymer complexes and their transitions with temperature and environment were studied by mixing curves, helix–coil transitions with temperature, and analytical buoyant density analyses.

(1) $(dA)_{12}$ OR $(rA)_{11} + (dT)_n$. The experimental mixing curve at 285 nm for $(dA)_{12}$ plus $(dT)_n$ fit the theoretical duplex curve for the samples above 50 mol % $(dA)_{12}$. If the assumption is valid that the 50 mol % $(dA)_{12}$ sample was duplex, then $(dA)_{12}$ forms duplex when it is in excess of the $(dT)_n$. However, the extinction coefficient at 285 nm calculated from the 50 mol % $(dA)_{12}$ sample is for that complex which is present in that sample. In reality, the theoretical 285-nm curve represents the variance with concentration of a structure(s), which might not necessarily be duplex. In any case, the complexes present in samples below 33 mol % and above 50 mol % $(dA)_{12}$ have different extinction coefficients at 285 nm.

The results of other analyses indicated that the dependence of the $(dA)_{12} \cdot (dT)_n$ complexes on stoichiometry was not as clear as the 285-nm mixing curve would indicate. First, mixing curves at 260 nm at 5° resembled those at 25°, with minimum absorbance at 33 mol % $(dA)_{12}$. At 40°, which was just at the lower edge of the major 260-nm melting transition, the point of maximum hypochromicity shifts to approximately 50 mol % $(dA)_{12}$. The $(dA)_{12} \cdot 2(dT)_n$ melting curve also showed that the triplex to single-strand transition had begun at 40°. Since the hypochromicity at 260 nm of the 50 mol % $(dA)_{12}$ sample at 40° was that expected for either complete duplex formation or for triplex plus single-strand $(dT)_n$, the structure(s) present must still have been stable.

Second, the melting transitions for $(dA)_{12} \cdot (dT)_n$ and $(dA)_{12} \cdot 2(dT)_n$ had distinctly different shapes. $(dA)_{12} \cdot 2(dT)_n$ behaved at 260 nm and at 285 nm as expected for a triplex to single-strand transition. If $(dA)_{12} \cdot (dT)_n$ was duplex, the depression seen in 285-nm curve would be expected for either a duplex to triplex or a duplex to single-strand transition. The transition that occurred above 50° at 260 nm that did not occur at 285 nm must be a triplex to single-strand transition. Classically, this means that the $(dA)_{12} \cdot (dT)_n$ complex must be undergoing a duplex to triplex to single-strand transition:

$$2[(dA)_{12} \cdot (dT)_n)] \longrightarrow (dA)_{12} \cdot 2(dT)_n + (dA)_{12} \longrightarrow 2(dA)_{12} + 2(dT)_n$$

The depression that occurred in the 260-nm curve is a structural transition which is not definable in terms of classical triplex or duplex complexes. Third, buoyant density analyses showed that in high ionic strength conditions, $(dA)_{12} \cdot (dT)_n$ and $(dA)_{12} \cdot 2(dT)_n$ formed essentially the same complex which was slightly less dense than polymer triplex.

In summary, $(dA)_{12} \cdot 2(dT)_n$ is apparently a classical triplex structure. $(dA)_{12} \cdot (dT)_n$ is neither a classical duplex nor triplex. $(dA)_{12} \cdot (dT)_n$ has triplex present, or the potential to form triplex when heated to 40° and higher or when the ionic strength is increased. The triplex-like structure that forms at 40° is slightly more stable than the $(dA)_{12} \cdot$

$2(dT)_n$ structure at the same temperature. When enough heat is added, the triplexes in both mixtures melt with the same T_m. The triplex might pass through a duplex structure in the process of melting, but this transition is too subtle to be detected by the melting curves even at 285 nm. The results for the $(dA)_{23}$ complexes follow the same trends. However, $(dA)_{23} \cdot (dT)_n$ forms a more duplex-like structure in neutral Cs_2SO_4 solution.

(2) $(dT)_{10} + (dA)_n$. Like the $(dA)_m$ structures, $(dT)_{10}$ structures also showed some dependency on stoichiometry as evidenced by the appearance of triplex in the mixing curve in TM buffer. That triplex does form with $(dT)_{10}$ was shown as follows.

(a) The melting curve of $(dT)_{10} \cdot (dA)_n$ in TM buffer consisted of two phases, where the more thermostable phase coincided with the transition for $2(dT)_{10} \cdot (dA)_n$.

(b) The buoyant density of $2(dT)_{10} \cdot (dA)_n$ was more dense than polymer duplex, but not as dense as polymer triplex. This behavior of the $(dT)_{10}$ complexes suggests that the propensity of an oligomer · polymer complex to be either triplex or duplex may depend in part on whether oligomer or polymer is the third strand found in the major groove of the duplex. A triplex with a polymer third strand would be expected to be more stable than a triplex with an oligomer third strand. In summary, a triplex structure can form with $(dT)_{10}/(dA)_n$ ratios of one or greater, but because the third strand is oligomer, it is probably a less stable structure than the $(dA)_m \cdot 2(dT)_n$ triplex.

More than one oligomer · polymer structure can be present in reaction mixtures at equilibrium. This study shows that the formation of triplex structures is dependent on oligomer length, is less favored when the third strand is oligomer, is favored by high ionic strength, and, finally, is influenced by stoichiometry, at least for the $(dA)_m$ and $(dT)_m$ complexes.

(3) GENERAL COMMENTS ON PHYSICAL DETERMINATIONS. None of the three determinations alone provided an unambiguous evaluation of the structures present under the polymerase reaction conditions. The interpretation of mixing curves assumes that complex formation is independent of stoichiometry and that complex formation is complete; neither of these assumptions was strictly valid for some cases studied herein. The major disadvantage of the A-T system was that the absorbance of triplex plus single strand, $(dA)_n \cdot 2(dT)_n + (dA)_n$, and the absorbance of the equivalent total concentration of duplex, $(dA)_n \cdot (dT)_n$, were essentially the same. For this reason, mixing curves also were read at 285 nm where the equivalent duplex and triplex plus single strand were distinguishable, but the extinction coefficients of duplex and of free $(dA)_n + (dT)_n$ were essentially equivalent. Using the 285-nm extinction coefficients calculated from the concentrations determined from the 260-nm curve, theoretical 285-nm curves were calculated and compared with the experimental curves.

Thermal denaturation curves also provide information on the types of structures present but their interpretation is complicated since structural rearrangements may take place as a function of temperature (e.g., Figure 5). Analytical buoyant density analyses must be performed in high salt concentration and hence provide values in an artificial environment; also, the high salt tends to stabilize triplex and thus provides an unrealistically high measure of the amount of triplex present in a complex (e.g., Figure 7). Likewise, since this is a time-consuming equilibrium measurement, a substantial time element is involved. If one of the components of a complex is readily dissociable and diffusable (i.e., $(dT)_{10}$ from $(dA)_n \cdot 2(dT)_{10}$), this measurement will give an unrealistically low density for a structure which was initially triplex (e.g., Figure 13). High-resolution nuclear magnetic resonance (NMR) currently is being explored as an alternate technique. Whereas it has certain inherent drawbacks, the in situ nature of the determination makes it promising.

Enzyme Effects. The results of the comparative enzyme assays also should be evaluated with respect to features of the DNA polymerases, namely (1) the presence of polymerase-associated nucleases and (2) enzyme stabilities and mechanisms.

(1) The first polymerase effect to be considered is the nuclease activity associated with each polymerase. The AMV polymerase used herein has RNase H activity (but no DNase activity) which is as potent as the DNA polymerase activity (Brewer and Wells, 1974). The presence of RNase H may explain why this polymerase did not utilize any ribo primers; one endo nick would destroy the ability of a ribooligomer to serve as primer.

Both the *M. luteus* polymerase and Pol I have 3′ to 5′ and 5′ to 3′ exonuclease activities (Harwood et al., 1970; Miller and Wells, 1972; Kornberg, 1969). Pol III has 5′ to 3′ and 3′ to 5′ single-strand specific exonuclease activities (Livingston and Richardson, 1975). The influence of the nucleases of the *M. luteus* polymerase would probably not be great on initial rates since the nuclease/polymerase ratio is about 1/100. Also, the *M. luteus* polymerase achieved approximately onefold synthesis before synthesis leveled off, which would indicate that nuclease activity was not a significant influence on net synthesis. However, the influence of nuclease would be more significant for Pol I, which has a higher nuclease/polymerase ratio (1/10 to 1). Prior studies (Sweet, 1972) showed that Pol I began to degrade labeled $(dT)_m$ primers at time zero, although net increases of synthesis and chain length were observed. The preferential utilization of some primers by Pol I may be due to the inability of the Pol I exonucleases to degrade them; however, the detailed nucleolytic studies necessary to substantiate nuclease preferences remain to be performed. Finally, the single-strand specific nucleases of Pol III may also influence synthesis by degrading the single-strand tails or the dissociated oligomer. However, since the nuclease/polymerase ratio is 0.3 (Kornberg and Gefter, 1972), this effect may be less important than the structural effects described above.

(2) All four polymerases have similar mechanisms (Kornberg, 1969; Miller and Wells, 1972; Green and Gerard, 1974; Gefter, 1974). The striking difference between the polymerases is that Pol III will make only an oligo product, whereas Pol I, the *M. luteus* polymerase, and the AMV polymerase can make a long polymer product. The influence of this difference on the ability of the polymerase to use certain primers is uncertain but is of significance with regard to the sensitivities of the assays. The observed product size may be more a function of enzyme stability than of differences in mechanisms. All the polymerases have finite half-lives at reaction temperatures, 25–37°, and most are stabilized in the presence of template · primers. In the presence of only triphosphates, the *M. luteus* polymerase and Pol I will remain at least partially active for many hours as shown by their ability to synthesize polymers de novo (Burd and Wells, 1970). Pol III loses 50% of its activity exponentially in 30 min at 25°, even in the presence of template

without triphosphates. It is much less stable than the other two enzymes. For Pol III, the rate of inactivation in the presence of all substrates could be directly related to how much time the polymerase is unbound relative to bound. If binding to substrate has a stabilizing effect, the rapid inactivation of Pol III would indicate that it must remain unbound more than the other polymerases. When much of the template · primer is unsuitable for elongation and binds polymerase without forming product, the amount of product formed per unit time will be even less. Binding to nonusable substrate and rapid loss of activity probably contribute to what has been called "gap specificity" (Kornberg and Gefter, 1972; Otto et al., 1973).

Acknowledgments

We thank J. Beard and D. Beard, Duke University, for AMV, P. Schendel and L. Brewer for the AMV DNA polymerase, M. Ryan for *E. coli* Pol I, J. Burd for help with the gel electrophoretic studies, and J. Larson for analytical ultracentrifuge analyses.

References

Adler, A., Grossman, L., and Fasman, G. D. (1967), *Proc. Natl. Acad. Sci. U.S.A. 57,* 423.

Baltimore, D., and Smoler, D. (1971), *Proc. Natl. Acad. Sci. U.S.A. 68,* 1507.

Brewer, L. C., and Wells, R. D. (1974), *J. Virol. 14,* 1494.

Burd, J. F., and Wells, R. D. (1970), *J. Mol. Biol. 53,* 435.

Burd, J. F., and Wells, R. D. (1974), *J. Biol. Chem. 249,* 7094.

Byrd, C., Ohtsuka, E., Moon, M. W., and Khorana, H. G. (1965), *Proc. Natl. Acad. Sci. U.S.A. 53,* 79.

Cassani, G. R., and Bollum, F. J. (1969), *Biochemistry 8,* 3928.

Chamberlin, M. J., and Patterson, D. L. (1965), *J. Mol. Biol. 12,* 410.

Chang, L. M. S., and Bollum, F. J. (1972), *Biochem. Biophys. Res. Commun. 46,* 1354.

Felsenfeld, G., and Miles, H. T. (1967), *Annu. Rev. Biochem. 36,* 407.

Flügel, R. M., and Wells, R. D. (1972), *Virology 48,* 394.

Gefter, M. L. (1974), *Prog. Nucleic Acid Res. Mol. Biol.,* 101.

Goodman, N. C., and Spiegelman, S. (1971), *Proc. Natl. Acad. Sci. U.S.A. 68,* 2203.

Green, M., and Gerard, G. F. (1974), *Prog. Nucleic Acid Res. Mol. Biol.,* 188.

Harwood, S. J., Schendel, P. F., and Wells, R. D. (1970), *J. Biol. Chem. 245,* 5614.

Hurwitz, J., and Wickner, S. (1974), *Proc. Natl. Acad. Sci. U.S.A. 71,* 6.

Keller, W. (1972), *Proc. Natl. Acad. Sci. U.S.A. 69,* 1560.

Kornberg, A. (1969), *Science 163,* 1410.

Kornberg, T., and Gefter, M. L. (1972), *J. Biol. Chem. 247,* 5369.

Leis, J. P., and Hurwitz, J. (1972), *J. Virol. 9,* 130.

Livingston, D. L., and Richardson, C. C. (1975), *J. Biol. Chem. 250,* 470.

Michelson, A. M., Massoulie, J., and Guschlbauer, W. (1967), *Prog. Nucleic Acid Res. Mol. Biol. 6,* 84.

Miller, L. K., and Wells, R. D. (1972), *J. Biol. Chem. 247,* 2667.

Morgan, A. R., and Wells, R. D. (1968), *J. Mol. Biol. 37,* 63.

Murray, N. L., and Morgan, A. R. (1973), *Can. J. Biochem. 51,* 436.

Nishimura, S., Jacob, T. M., and Khorana, H. G. (1964), *Proc. Natl. Acad. Sci. U.S.A. 52,* 1494.

Otto, B., Bonhoeffer, F., and Schaller, H. (1973), *Eur. J. Biochem. 34,* 440.

Riley, M., Maling, B., and Chamberlin, M. J. (1966), *J. Mol. Biol. 20,* 359.

Sweet, R. W. (1972), Ph.D. Thesis, University of Wisconsin.

Uhlenbeck, O. C. (1969), Ph.D. Thesis, Harvard University.

Verma, I. M., Meuth, N. L., and Baltimore, D. (1972), *J. Virol. 10,* 622.

Wartell, R. M., Larson, J. E., and Wells, R. D. (1974), *J. Biol. Chem. 249,* 6719.

Weiss, B., Live, T. R., and Richardson, C. C. (1968), *J. Biol. Chem. 243,* 4530.

Wells, R. D., Flügel, R. M., Larson, J. E., Schendel, P. F., and Sweet, R. W. (1972), *Biochemistry 11,* 621.

Wells, R. D., and Inman, R. B. (1973), DNA Synthesis in Vitro, Baltimore, Md., University Park Press.

Wells, R. D., and Larson, J. E. (1972), *J. Biol. Chem. 247,* 3405.

Wells, R. D., Larson, J. E., Grant, R. C., Shortle, B. E., and Cantor, C. R. (1970), *J. Mol. Viol. 54,* 465.